TISSUE ENGINEERING: Part A
Volume 16, Number 1, 2010

DOI: 10.1089/ten.tea.2008.0550

# Formation of Human Capillaries *In Vitro*: The Engineering of Prevascularized Matrices

Irene Montaño, Ph.D., Clemens Schiestl, M.D., Jörg Schneider, M.D., Luca Pontiggia, Ph.D., Joachim Luginbühl, M.S., Thomas Biedermann, M.S., Sophie Böttcher-Haberzeth, M.D., Erik Braziulis, Ph.D., Martin Meuli, M.D., and Ernst Reichmann, Ph.D.

Initial take, development, and function of transplanted engineered tissue substitutes are crucially dependent on rapid and adequate blood perfusion. Therefore, the development of rapidly and efficiently vascularized tissue grafts is vital for tissue engineering and regenerative medicine. Here we report on the construction of a network of highly organotypic capillaries in engineered tissue substitutes. We employed a three-dimensional culture system consisting of human microvascular endothelial cells. These were reproducibly expanded at high purity and subsequently seeded into biodegradable, fibrin-based hydrogels. The process of capillary formation *in vitro* followed the principles of both angiogenesis and postnatal vasculogenesis and a distinct sequence of other developmental steps that closely resemble embryonic neovascularization. Capillary lumen formation *in vitro* was initiated by the deposition of a basement membrane and intensive pinocytosis, followed by the generation of intracellular vacuoles, successive fusion of these vacuoles, and finally the formation of a long, continuous lumen. After transplantation the vascular structures were stabilized by mural cells of the recipient animal. Our findings suggest that the *in vitro* engineering of prevascularized matrices is within reach.

## Introduction

Without an adequate vascular (supply) system not even plane tissues (such as skin), let alone more voluminous tissues (such as muscle or parenchymous organs), will survive and thrive after transplantation.[1]

It is well known, however, that full-thickness skin (1–3 mm thick) is rapidly perfused after transplantation.[2–6] Young *et al.* have described three mechanisms responsible for graft survival and the establishment of blood supply of human full-thickness skin, which are as follows: (1) diffusion of nutrients through the graft (imbibition), (2) neovascularization,[7] and (3) and inosculation. Diffusion through the dermis is just too inefficient to allow survival of the epidermis. Neovascularization (by angiogenesis and vasculogenesis) occurs with a large delay and therefore is not the critical mechanism that keeps a transplant alive early after transplantation. Inosculation is the formation of anastomoses between graft and recipient vessels. As inosculation occurs rapidly, it guarantees survival of the graft early after transplantation. Thus, rapid inosculation of an *in vitro* prevascularized, autologous graft is what we envision in this project.

Recent advances in understanding the process of blood vessel development have offered important tools for therapeutic neovascularization. Basically three approaches have been attempted for vascularization of bioengineered tissue: (1) incorporation of soluble angiogenic factors, (2) gene transfer approaches,[8,9] and (3) seeding of endothelial cells onto or into matrices and scaffolds.[2,10–13] Of these, the latter one turned out to be most promising. Numerous matrices and scaffolds have been used to study vessel formation under controlled conditions. However, the heterogeneity of the conditions used makes it difficult to compare findings between different laboratories. Models of vasculogenesis and angiogenesis vary in endothelial cell type, number of endothelial cells, types and concentrations of matrix components, composition of soluble factors, and the time period the cells were exposed to these conditions. Hardly any of these assays closely recapitulates the *in vivo* process, and only few models were designed for clinical use. This is also reflected by the fact that in most of these models, animal endothelial cells or human umbilical vein endothelial cells (HUVECs) were used. Autologous HUVECs, however, are still rarely available in a clinical setting.

We show here that the human dermis is a perfect source of microvascular endothelial cells that can be expanded in a reproducible manner in culture. Further we demonstrate that vasculogenesis and angiogenesis can occur *in vitro* under

Tissue Biology Research Unit, Department of Surgery, University Children's Hospital, University of Zurich, Zurich, Switzerland.

appropriate conditions and that the construction of true three-dimensional (3D) capillary networks, hence the *in vitro* engineering of prevascularized interstitial matrices, is within reach. In a second phase we transplanted these prevascularized matrices onto the backs of immunoincompetent rats (see also our recent work[14]) and showed that mural cells recruited from the underlying recipient mesenchyme stabilized the engineered vessels.

## Materials and Methods

### *Isolation of microvascular endothelial cells*

Human microvascular endothelial cells (HuMECs) were isolated from human foreskins obtained from the University Children's Hospital of Zurich after routine circumcisions and stored in Dulbecco's modified Eagle's medium (Invitrogen, Basel, Switzerland) supplemented with 1.5 μL/mL gentamycin, 30 μL/mL PenStrep, and 1 μL/mL fungizone. All patients (and/or their parents) gave their written consent for this study in accordance with the Ethics Commission of the Kanton Zurich (notification no. StV-12/06). Foreskins were cut into approximately 1 $cm^2$ pieces and incubated with 75 U/mL collagenase type II (Worthington, Lakewood, NY) at 37°C for 1 h. HuMECs were harvested by scraping the dermal side with the back of a scalpel blade. The cell suspension was centrifuged at 170 *g* for 10 min and the cell pellet was resuspended in microvascular endothelial cell growth medium-2 (EBM-2 MV; Lonza, Basel, Switzerland) with supplements (Lonza, CC-4147). HuMECs were grown on 1% gelatine-coated culture dishes in 5% $CO_2$ at 37°C. The medium was changed three times a week. The cells were used at passage 1 in all experiments.

### *Preparation of prevascularized fibrin matrices*

Fibrinogen from bovine plasma (Sigma-Aldrich, Buchs, Switzerland) was used for the preparation of fibrin gels. Fibrinogen was reconstituted in NaCl according to the instructions of the provider to a final concentration of 7, 9, 10, 11, 13, and 15 mg/mL. To 1 mL of fibrinogen solution, $1\times10^4$, $3\times10^4$, $5\times10^4$, $1\times10^5$, $2\times10^5$ cells and 22 μL thrombin (Sigma-Aldrich, 50 U/mL) were added and seeded in an insert for six-well plates. After clotting at room temperature, the preparations were incubated at 37°C for 1 h in a humidified incubator containing 5% $CO_2$ to ensure polymerization of fibrin. At the end of the incubation period, EBM-2 MV was added to the upper and lower chambers, and gels were incubated for 3 weeks until transplantation. To prepare randomly distributed single Endothelial cells (ECs) in fibrin gels, a single-cell suspension of 100,000 cells was submerged within 1 mL of a fibrin gel and this gel was transplanted right away.

### *Preparation of collagen type I hydrogels*

Collagen type I hydrogels at final concentrations of 2.5, 3.0, and 3.5 mg/mL were prepared using collagen type I (5 mg/mL; Symatese, Chaponost, France). Polymerization of the acidic soluble collagen was reached by adding reconstitution solution that contained 6 mg/mL NaOH. The culture medium was added 30 min after polymerization.

Lyophilized collagen "sponges" or artificial skin were provided by (Matricel, Herzogerath, Germany), EMCM (The Netherlands), Symatese, and (Integra Life Sciences, Geneva, Switzerland).

### *Grafting to athymic rats*

Animal studies were performed with the approval of the Institutional Animal Care of the University of Zurich following the guidelines of the National Institutes of Health.

Immunoincompetent female Nu/Nu rats (Elevage Janvier) were anaesthetized by inhalation of 5% isofluran (Baxter, Volketswil, Switzerland) and narcosis maintained by inhalation of 2.5% isofluran via mask. Before the operation, 0.5 mg/kg buprenorphin (Temgesic®; Essex, Luzern, Switzerland) for analgesia and retinol cream (Vitamin A "Blache"®; Bausch & Lomb, Berlin, Germany) for eye protection were applied. To prevent wound closure from the side, a special polypropylene ring, 2.6 cm in diameter, was designed in our laboratory. The rings were sutured to full-thickness skin defects created on the back of the rats using nonabsorbable polyester sutures (Ethibond®; Ethicon, Norderstedt, Germany).

Cultured fibrin gels ($n = 5$ per group) were placed into the polypropylene rings and covered with a silicon foil (Silon-SES; BMS) and polyurethane sponges (Ligasano®; Ligamed, adolzbufe, Germany). Controls with unorganized HuMECs and empty gels were included.

Rats were sacrificed at 5 days and 2 weeks after surgery. At sacrifice, dressings and sutures were removed and multiple graft biopsies were collected for different analyses.

### *Histological analyses*

Skin equivalents were fixed in 4% neutral formalin and embedded in paraffin according to the standard protocols. The 6 μm sections were cut and stained using Mayer's hematoxylin and eosin solution (both from Sigma-Aldrich).

### *Immunohistochemical analyses*

Biopsies were embedded in Tissue Tek. Cryosections (10 μm) were fixed for 5 min in acetone–methanol at −20°C and blocked for 30 min in 2% normal goat serum in phosphate-buffered saline (PBS) before antibody incubation. The following primary antibodies were used: rabbit anti-human von Willebrand factor (vWf) (DakoCytomation; 1:100, Baar, Switzerland), monoclonal mouse anti-human CD31 (DakoCytomation; 1:40), mouse anti-SMA (DakoCytomation; 1:100), rabbit anti-laminin 1 + 2 (Abcam, Cambridge, MA), monoclonal mouse anti-human CD90 (Thy-1), and clone AS02 (Dianova; 1:100, Hamburg, Germany). This antibody reacts specifically with human CD90 (Thy-1), a glycosyl-phosphatidyl-inositol (GPI)-anchored glycoprotein that is expressed in various types of human fibroblasts (see Supplemental Fig. S1, available online at www.liebertonline.com/ten). Secondary antibodies used were as follows: Fluorescein-isothiocyanat (FITC)-conjugated polyclonal goat F(ab′)2 fragments directed to mouse immunoglobulins (DakoCytomation), FITC-conjugated polyclonal swine F(ab′)2 fragments directed to rabbit immunoglobulins (DakoCytomation), Tetramethylrhodamine-5-isothiocyanat (TRITC)-conjugated polyclonal rabbit directed to mouse immunoglobulins (DakoCytomation), and FITC-conjugated polyclonal rabbit directed to goat immunoglobulins (DakoCytomation). All

antibodies were incubated at 37°C for 1 h. Nuclei were counterstained with Hoechst. All slides were mounted with fluorescent mounting medium (DakoCytomation). For the staining of the paraffin-embedded samples, antigen retrieval was performed (Dako Target retrieval solution).

Specificity of human cell markers was confirmed by the absence of any signal in untransplanted control animals. In addition, omission of the first antibody was used as a negative control. Immunocytochemistry was also used to confirm the identity of HuMECs in culture using the monoclonal antibody against the endothelial cell marker CD31.

### In situ *hybridization*

DNA labeling with digoxigenin. Human genomic DNA of a free volunteer was extracted with the QIAamp DNA Blood Midi Kit (Qiagen, Basel, Switzerland). The polymerase chain reaction (PCR) primers were positioned in the most conserved areas of human Alu sequences and produced a PCR product of 245 bp using the modified method of Just *et al.*[15] Modifications were as follows. For PCRs, following primers for Alu sequences were used:

Alu-sense: 5′ ACG CCT GTA ATC CCA GCA CTT 3′

Alu-antisense: 5′ TCG CCC AGG CTG GAG TGCA 3′

PCR was carried out under the following conditions: 94°C for 10 min, 30×(94°C for 30 s, 58°C for 45 s, 72°C for 45 s) and 72°C for 10 min. PCR products were electrophoresed on a 2% agarose gel and stained with ethidium bromide [1.5 μg/mL in 1× tris-acetate-EDTA (TAE)]. DNA band of 245 bp was eluted with the high pure PCR product purification kit (Roche, Basel, Switzerland). The PCR product was digoxigenin (DIG) labeled with the PCR DIG probe synthesis kit (Roche). This PCR was performed with 50 ng eluted DNA by using the same PCR protocol, as described above. The labeled probe was purified by ethanol precipitation according to the protocol of PCR DIG probe synthesis kit.

In situ hybridisierung (ISH) on paraffin sections. Paraffin sections (5 μm) were mounted on silane-coated slides (Sigma-Aldrich) and dried overnight at 37°C. Sections were deparaffinized in xylene, rehydrated in a graded ethanol series, and air dried. The protocol followed is based on the method described by Just *et al*. with some modifications.[15] After three washes for 5 min with PBS (0.1 mM, pH 7.4), slides were incubated with PBS containing 0.3% Triton® X-100 for 10 min. Slides were then incubated with tris-EDTA (TE) buffer containing 2 μg/mL proteinase K, for 25 min at 37°C and rinsed again three times for 5 min in TE buffer. To reduce nonspecific background, slides were acetylated using TEA buffer (0.1 M triethanolamine, pH 8.0) containing 0.25% (v/v) acetic anhydride (Sigma) twice for 5 min. After prehybridization with hybridization buffer (50% formamide [Sigma-Aldrich] in 5×saline-sodium citrate (SSC), 0.1% sodium/lauroylsarcosine [Sigma], 0.02% SDS [Sigma], 2% blocking reagent [Roche]) for 150 min at 85°C, slides were incubated with fresh hybridization buffer containing the denatured DIG-labeled DNA probe (100 ng/mL) for further 2 h at 85°C. After that slides were immediately transferred to ice for 10 min and then incubated overnight at 42°C. Prehybridization and hybridization steps were performed in a moist chamber containing 50% formamide. After hybridization, slides were briefly rinsed in 2×SSC at room temperature and three times in 0.1×SSC for 15 min at 42°C. Observation of the hybridized DNA probe was performed according to the protocol of the DIG nucleic acid detection kit (Roche). The slides were incubated with alkaline phosphatase–conjugated antibody solution (1:2000 in blocking buffer [1% blocking reagent; Roche] containing 0.1% Triton X-100) for 1 h, following four washes with maleic acid buffer (0.1 M maleic acid, 0.15 M NaCl, pH 7.5) for 15 min. Slides were equilibrated for 5 min in Tris buffer pH 9.5 (0.1 M Tris, pH 9.5, 0.1 M NaCl, 50 mM $MgCl_2$). The color development was carried out with freshly prepared substrate solution (nitroblue tetrazolium salt and 5-bromo-4-chloro-3-indolyl phosphate (X phosphate) (Roche) in Tris buffer (pH 9.5). After 15 to 30 min, the enzymatic reaction was terminated with stop buffer (10 mM Tris/HCl, pH 8.0, 1 mM ethylenediaminetetraacetic acid). Slides were washed three times for 15 min and incubated with phosphate-buffered Hoechst solution (1 μg/mL) for 15 min. Finally, slides were rinsed three times with PBS.

### *Transmission electron microscopy*

The gels containing the vascular structures were fixed in 50 mM sodium cacodylate buffer, pH 7.3, containing 2% glutaraldehyde and 0.8% paraformaldehyde and postfixed with 1% $OsO_4$ in 50 mM sodium cacodylate buffer, pH 7.3, dehydrated in an ethanol series and embedded into epon (Catalys). Ultrathin sections of 50 nm were contrasted with uranyl acetate and lead citrate and studied with a CM 100 transmission electron microscope (Phillips, Zurich, Switzerland).

### *Light microscopy*

Capillaries were viewed at distinct stages of graft formation and posttransplantation by both epi-illuminated stereomicroscopy and inverse light microscopy.

## Results

### *Vascular structures develop in a fibrin-based hydrogel*

We prepared HuMECs from 32 different foreskins. The foreskins were derived from children and young adults ranging in age from newborn to 18 years old. There were two foreskins from newborns. We consider the cells derived from 15, 17, and 18-year-old patients as adult cells. We have shown in 23 distinct experiments that HuMECs isolated from all categories of patients mentioned above can develop into lumenized vascular structures within fibrin hydrogels. To harvest maximal numbers of HuMECs at high purity, a novel procedure was developed. With this method it became possible to rapidly isolate CD31 (PECAM1)-positive HuMECs from human skin biopsies at about 98% purity (Fig. 1A and Supplemental Fig. S1). Thus, an additional enrichment of HuMECs by fluorescence-activated cell sorting (FACS) or magnetic cell separation (MACS) was not necessary. Further, we developed collagen and fibrin-based biodegradable matrices to screen for optimal 3D organotypic structure formation. We tested fibrin hydrogels at concentrations of 7, 9, 10, 11, 13, and 15 mg/mL. In addition, collagen hydrogels at final concentrations of 2.5, 3.0, and 3.5 mg/mL were examined. Finally, collagen/fibrin composite hydrogels mixed at concentrations (fibrin + collagen) of 7 + 3 mg/mL, 9 + 3 mg/mL,

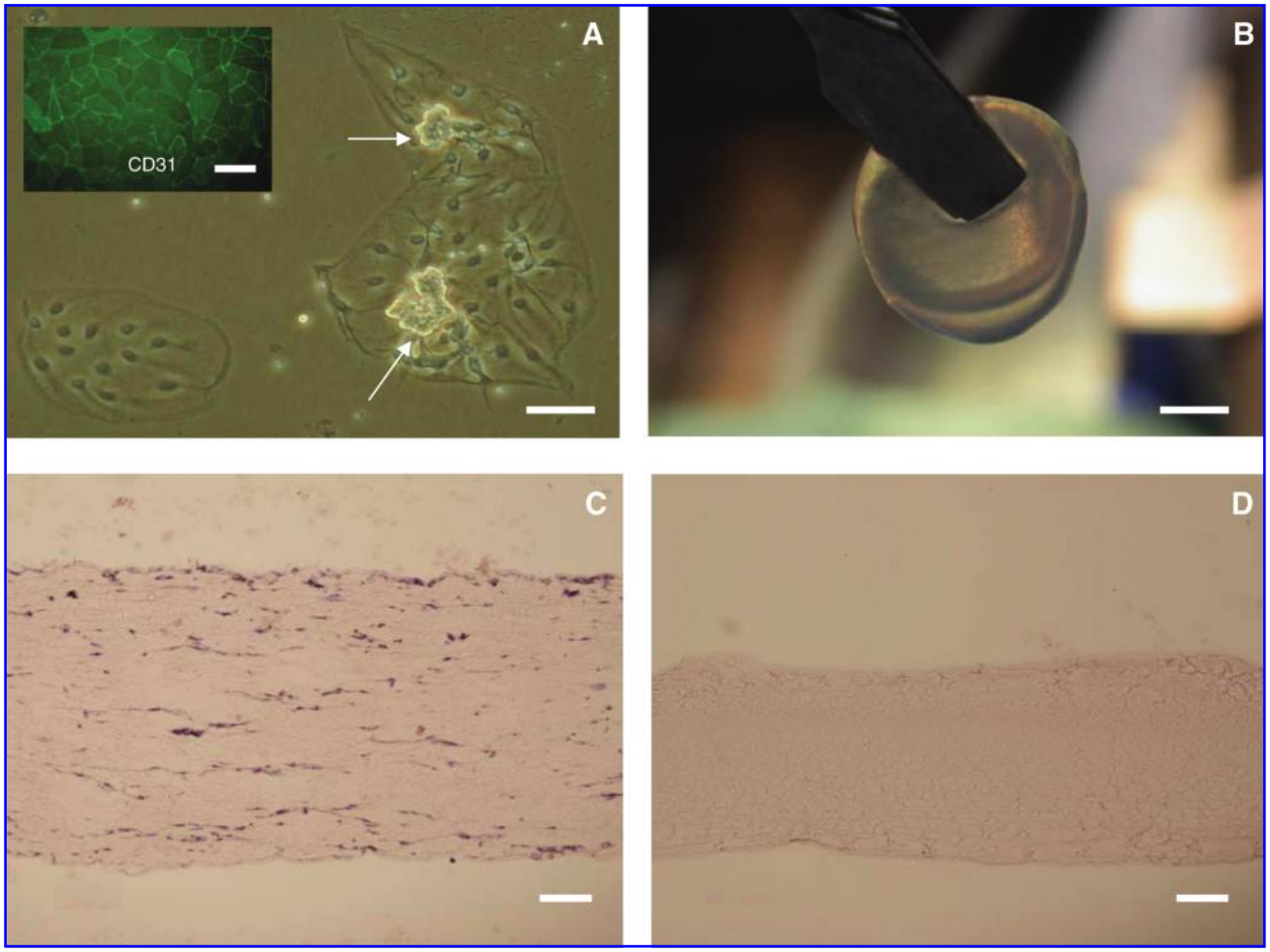


**FIG. 1.** Highly enriched HuMECs submerged within a novel biodegradable matrix. (**A**) HuMECs derived from dermis growing out from capillary fragments (arrows) on cell culture plastic. CD31 (PECAM) expression confirms the endothelial origin of the cells (inset). (**B**) The fibrin-based matrix remains stable in size and pliability after vascular structures have developed (3 weeks in culture). (**C**) Vascular structures thicken and stabilize the hydrogel. (**D**) The acellular hydrogel is thinner and significantly less stable than the prevascularized gel. Scale bars in (**A**) 50 μm; (**B**) 1 cm; (**C**); and (**D**) 100 μm. HuMEC, human microvascular endothelial cells. Color images available online at www.liebertonline.com/ten.

and $10+3$ mg/mL were investigated. Among the tested matrices, only fibrin-based hydrogels at concentrations of 10 and 11 mg/mL allowed the formation of true 3D and lumenized vascular structures. Other fibrin concentrations turned out to be suboptimal, leading to short cords or irregular cell aggregates that did not exhibit lumen formation and showed only moderate branching (data not shown). Similarly, in collagen hydrogels, HuMECs remained mostly as spherical aggregates or as very short cords (data not shown). Under these conditions neither branching nor lumen formation was observed. In fibrin/collagen hybrid gels, few extended and branching cords were observed. However, lumen formation was not possible (data not shown). Thus, the *in vitro* development of branching and lumenized vascular structures was only possible in a limited density of reconstituted fibrin matrix.

All fibrin gels were initially 1 mm thick. This matrix did not shrink *in vitro* and could be conveniently handled during surgical interventions (Fig. 1B). Moreover, the presence of vascular structures had a clear effect on the stability of the fibrin matrix. The preformed vascular structures clearly contributed to the thickness and stability of the substitute. Without vascular structures the gel had an increased fluidity, which on the one hand increased its radius and on the other hand decreased its thickness. (Fig. 1C, D) We did not observe significant degradation of the fibrin gels *in vitro* because the numbers of fibroblasts were low or zero.

The 3D distribution of HuMECs within the biodegradable matrix, and hence its homogeneous population by vascular structures, was achieved upon submerging the cells in the rapidly polymerizing matrix. Rapid polymerization was crucial, since it forced the HuMECs to stay firm in their different planes and 3D positions. By this procedure their sedimentation and accumulation in only one plane (two-dimensional), that is on the underlying porous membrane, was avoided. As a result HuMECs evenly distributed in three dimensions developed into clusters of proliferating endothelial cells. Importantly, within about 5 days these cells gave rise to branching organotypic structures consisting of single, elongated cells (Fig. 2A). Apparently a sufficient number of precursor cells was present in our preparations of dermal HuMECs to permit vasculogenesis *in vitro*. At about

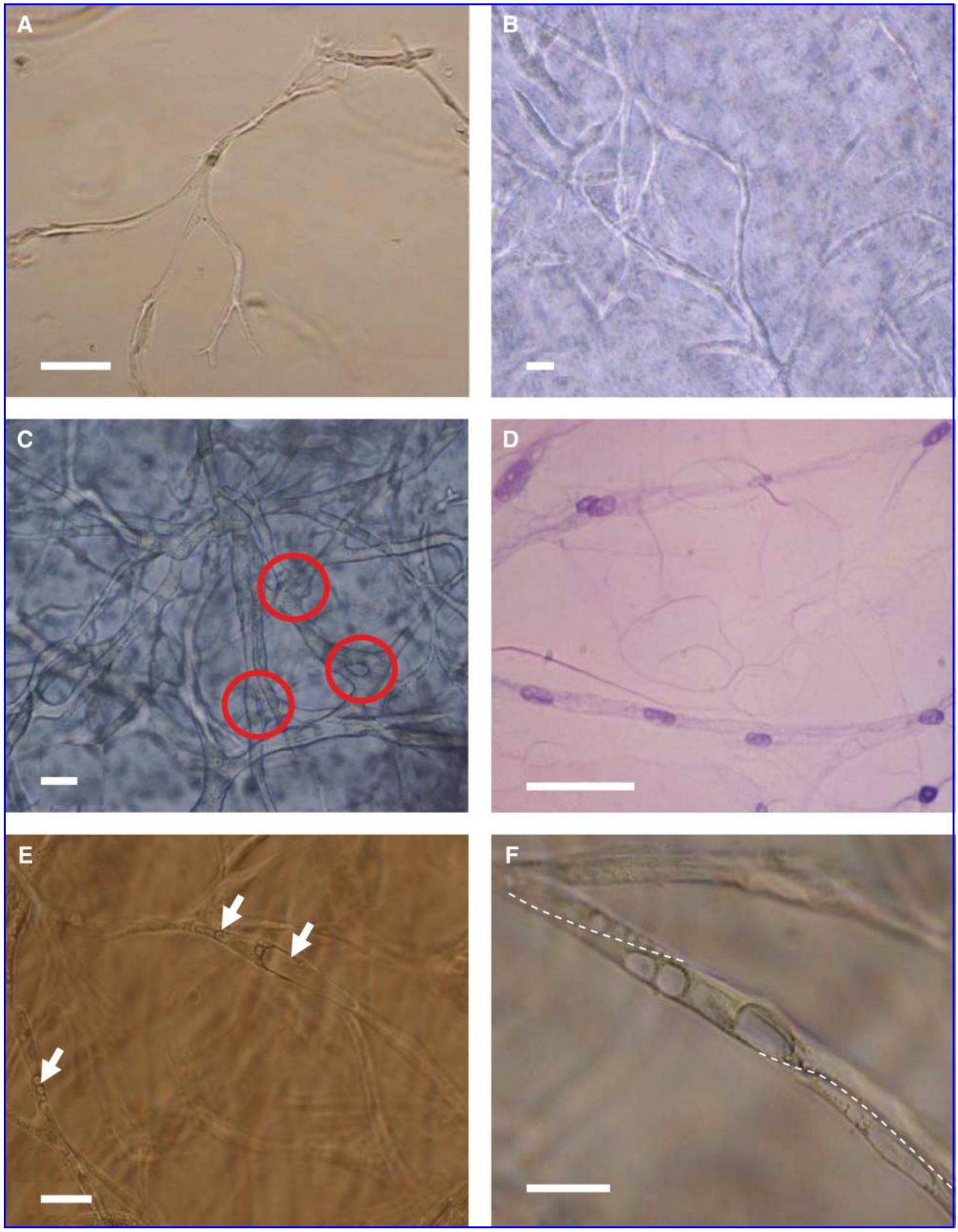


**FIG. 2.** The distinct steps of capillary formation *in vitro*. (**A**) Single HuMECs assemble into faint branching cords 5 days after submerging them into fibrin-based hydrogels of approximately 1 mm thickness. (**B**) Vascular structures forming after 7 days in culture. (**C**) Dependent on the number of initially plated cells, HuMECs develop into dense networks of branching solid cords. Anastomoses are indicated by circles. (**D**) Histological analyses (HE staining) 10 days after plating reveal that the developing structures comprise solid cords. Note the cytoplasmatic hematoxylin staining that indicates that no lumen has formed yet. (**E**) Successively arranged vacuoles (arrows) undergo fusion to form increasing lumens in vascular structures. (**F**) Three vacuole-forming HuMECs aligning in an overlapping fashion. Cell borders are indicated by dotted lines. All scale bars: 50 μm. HE, hematoxylin and eosin. Color images available online at www.liebertonline.com/ten.

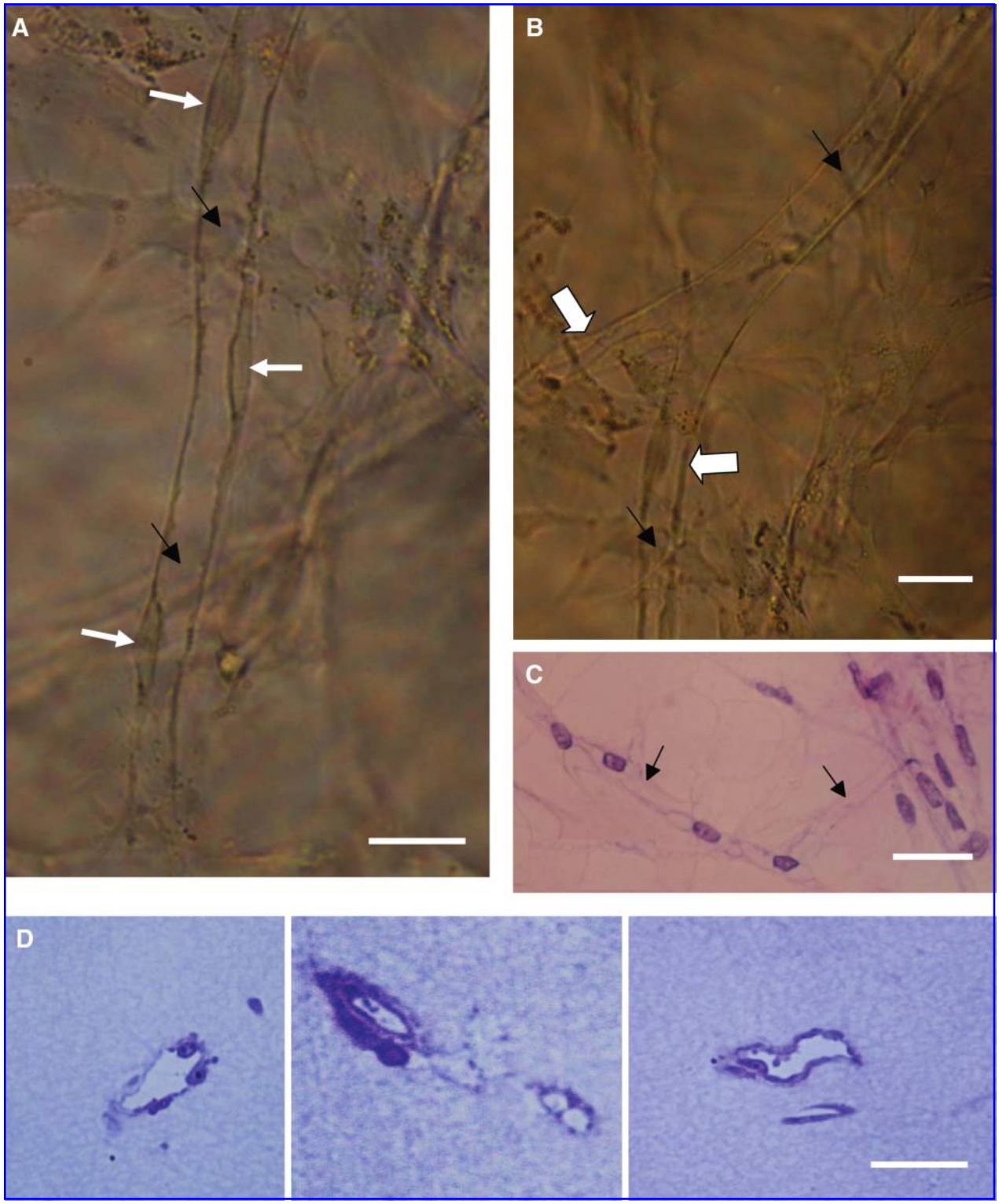


**FIG. 3.** Phase-contrast microscopy of branching, completely lumenized capillaries developing in hydrogels *in vitro*. (**A**) Regularly alternating nuclei (white arrows) and the cytoplasm are closely associated with the plasma membrane. Black arrows indicate the lumen. (**B**) The two branches of a capillary are indicated by white arrows. Black arrows indicate the lumen. (**C**) Histological sections and HE staining reveal that almost all vascular structures exhibit a lumen 25 days after plating. Black arrows indicate the lumen. Note that the lumen is free of hematoxylin staining. (**D**) A series of cross sections through lumenized capillaries that have developed in fibrin hydrogels. Sections were counterstained with toluidine blue. Scale bars in (**A**) and (**B**) 10 μm, and in (**C**) and (**D**) 30 μm. Color images available online at www.liebertonline.com/ten.

7–10 days after cell plating, the vascular structures became longer and stronger and developed into solid branching cords (Fig. 2B). Dependent on the number of the initially plated endothelial cells, the structures extended into real networks. Here anastomoses were obvious (Fig. 2C, circles). Histological analyses revealed that at this stage HuMECs had arranged into a network of solid cords and lumen formation was not detected in any of the structures (Fig. 2D). The optimal cell number was $3\times10^4$ cells per mL of gel. At very high cell numbers (e.g., $2\times10^5$ cells per mL), numerous and very thin cords occurred (data not shown). These structures obviously were in competition for growth factors and nutrients, so that the development of normally sized cords and a subsequent lumen formation was not possible. At low cell concentrations (5000–10,000 cells/mL), some spot wise, focal outgrowth of vascular structures occurred. In these structures, large vacuoles were frequently detectable, while formation of a continuous lumen was rare (data not shown).

### *Vacuoles fuse to form a lumen*

About 15 days after plating, rows of successively arranged vacuoles became evident in most of the cords. In addition, short stretches of fused vacuoles became visible representing the first lumenized segments (Fig. 2E, arrows). The fusion process did not occur synchronously throughout the vascular structure but was rather initiated in certain spots within the structure. However, lumen formation occurred in 70–80% of the vascular structures in one gel. Figure 2F shows three adjacent elongated cells overlapping at their ends. Phase-contrast light microscopy revealed that some vacuoles within one cell fused to form a larger vacuole. Light microscopy, however, could not reveal whether lumen formation just occurred in the cytoplasm of individual cells or whether the lumen developed in the intercellular space. After about 20 days in culture, highly organotypic, branching capillaries had developed with nuclei positioned at their faint cell membranes (Figs. 3A–C). Finally, a network of branching and interconnected capillaries had developed (Figs. 3B, C).

Although lumen formation was obvious by phase-contrast microscopy, we performed histological analyses that revealed the presence of a complete lumen in 70–80% of the structures (Fig. 3C). Notably, no mural cells, such as pericytes and vascular smooth muscle cells, were attached to the capillaries (Fig. 3A–C). Lumen formation was also shown by a series of cross sections through lumenized capillaries grown in fibrin hydrogels (Fig. 3D). These findings indicate that a network of simple human capillaries can be generated *in vitro*.

### *Transmission electron microscopy and immunofluorescence data reveal that lumen formation occurs according to the cord hollowing mechanism of tubulogenesis*

To gain additional insight into the mechanism of lumen formation, electron microscopical analyses were performed. In Figure 4A two elongated HuMECs after 2 days in a fibrin gel are depicted. The optimal density of fibrin fibers that ideally supports capillary formation is shown. A basement membrane (BM) is not yet deposited. As HuMECs form contacts and develop into branching cords (shown in Fig. 2), they also start to interact with their extracellular environment. Two important processes take place. First, a BM is produced (black arrows in Fig. 4B, C). The deposition of a BM was always detected in ECs that arranged into vascular structures in fibrin hydrogels. The BM instructs the endothelial cells to polarize, which is the establishment of a basolateral and an apical (luminal) membrane domain. Apparently without apical and basolateral polarization, no lumen formation is possible. Second, extensive pinocytosis (cell drinking) is observed in all samples investigated (Fig. 4B, C, white arrows). Vesicles invaginating from the plasma membrane are taken up by the cytoplasm, and obviously these vesicles are fusing to form large intracellular vacuoles (Fig. 4C, filled gray arrows). Deposition of BM components 15 days after plating is confirmed by immunofluorescence employing laminin $1+2$ and CD31 antibodies (Fig. 4D–G). All cells of the *in vitro* engineered vascular structure are CD31 positive (Fig. 4E). The nuclei of this structure are arranged around the lumen, as revealed by Hoechst staining (Fig. 4F). The merger of the three afore-mentioned immunostainings is shown in Figure 4G. Figure 4H illustrates that the lumen develops in the intercellular space, which is always free of matrix material. We consider it likely that the intracellular vacuoles fuse with the luminal (apical) membrane to increase the lumen. Hence, as the lumen forms, the participating endothelial cells have completed their polarization process, exhibiting an apical (luminal) and a basolateral domain. In this stage of capillary development, a BM can be detected (Fig. 4H, magnified inset). Finally, the initially solid cell cords have developed a central lumen (Fig. 4I). At this stage the cytoplasm and the nuclei become gradually more associated with the outer, basolateral plasma membrane.

The scheme shown in Figure 5 is based on our electron microscope (EM) data and light microscopical observations and depicts the distinct steps of lumen formation. Notably, the mechanism described here is in line with the cord hollowing mode, which implies that a lumen is created *de novo* in the intercellular space between polarizing cells within a cylindrical cord.[16]

### *Engineered vascular structures are stabilized* in vivo

To assess the therapeutic potential of our approach, we analyzed integration, stabilization, and survival of the transplants in animal studies. Prevascularized matrices were grafted onto full-thickness skin wounds of 2.6 cm diameter on 8–10 weeks old immunoincompetent Nu/Nu rats in six independent sets of experiments.

Three types of grafts were analyzed: (1) gels without cells, (2) gels containing single, randomly distributed HuMECs, and (3) gels in which HuMECs had developed into lumenized capillaries. We wanted to investigate whether the presence of single ECs already had an effect on the vascularization of the gels after transplantation (as compared to acellular gels). In addition we decided to study whether there was a difference in vascularization between prevascularized gels that may rapidly connect to the underlying vascular network and gels containing randomly distributed HuMECs (but no preformed capillaries) that had no chance to rapidly connect to underlying vascular structures of the recipient animal.

Hematoxylin and eosin staining revealed the thickness and structure of the fibrin gel that did not contain cells before

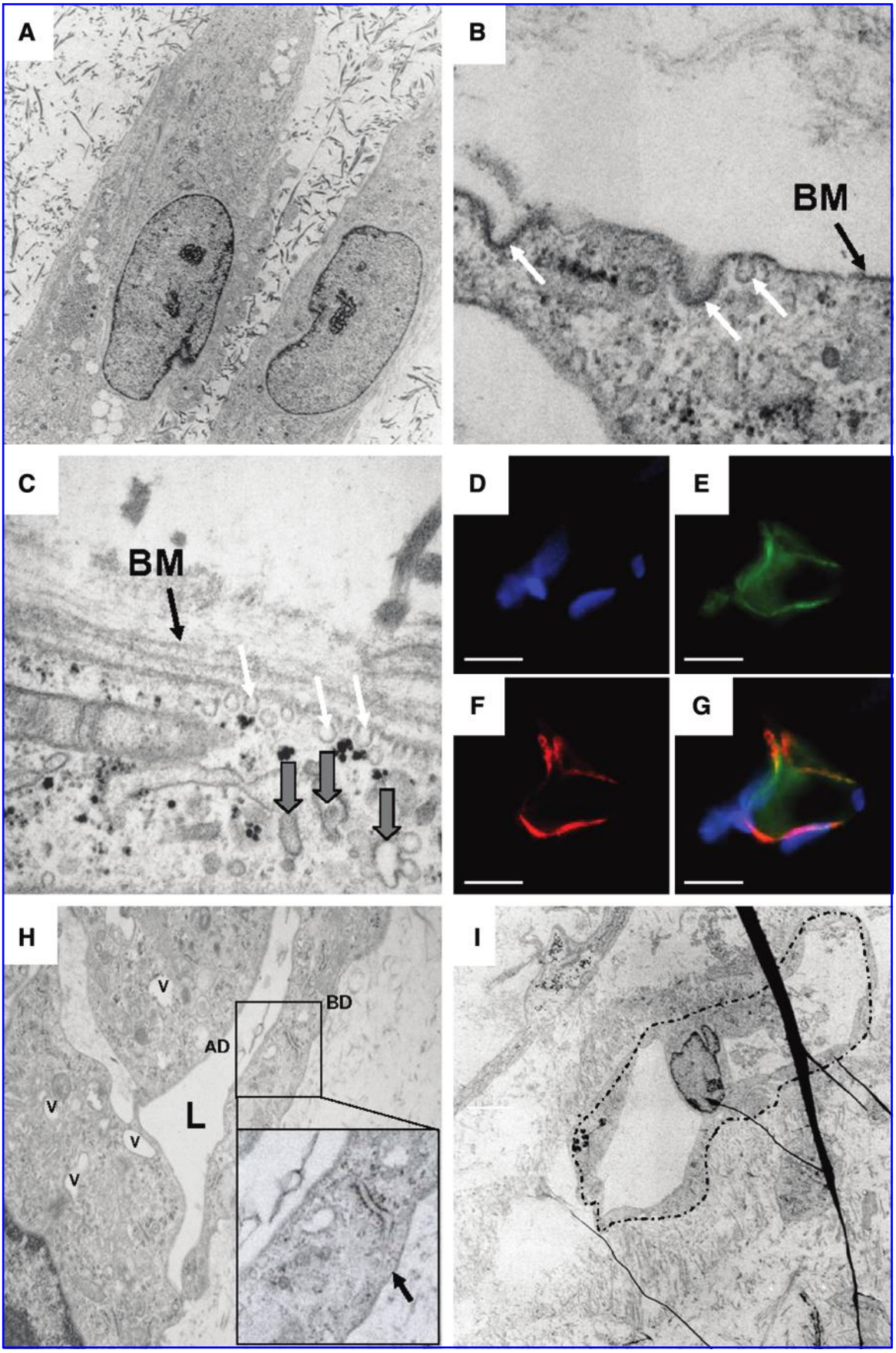
A
B
BM
C
BM
D
E
F
G
H
V
BD
AD
L
V
V
V
I

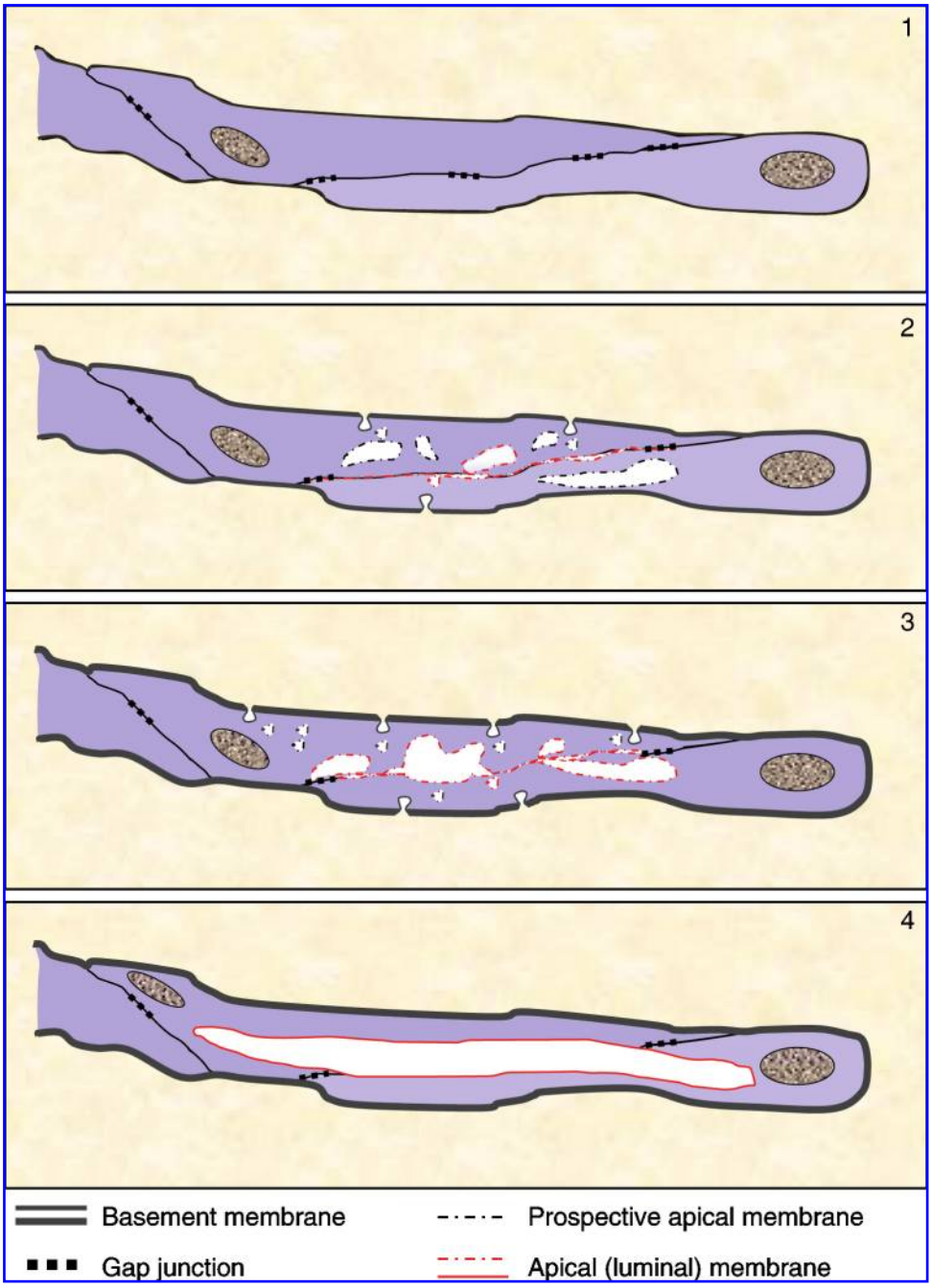


**FIG. 5.** A model based on our findings depicting the distinct steps of endothelial lumen formation in our *in vitro* system. Our observations greatly favor the cord-hollowing hypothesis: (**1**) Aggregation of single ECs into solid cords is mediated by junctional complexes. Contact with the extracellular matrix determines the basolateral membrane domain. (**2**) An "early" BM is deposited. The beginning pinocytotic activity (vesicle invaginations) results in the formation of intracellular vacuoles that are lined by the prospective apical membrane (black dotted line) or by the (final) apical membrane (red dotted line). (**3**) A lumen is created *de novo* in the intercellular space of polarizing ECs. Pinocytosis is fully active. The BM is further completed. (**4**) Vacuole fusion results in the formation of the lumen in the intercellular space of two ECs. Endothelial cell polarity is fully established. Color images available online at www.liebertonline.com/ten.

**FIG. 4.** EM analyses reveal the critical implication of cell–cell and cell–matrix adhesion in the establishment of cell polarization and intercellular lumen formation after submersion in a fibrin gel. (**A**) HuMECs for 2 days in a fibrin matrix. A basement membrane (BM) cannot be recognized yet. (**B**) Seven days after plating, a BM starts to be deposited, and invaginating vesicles (white arrows) are visible. (**C**) Numerous invaginating vesicles (white arrows) indicate extensive pinocytosis (cell drinking) 10 days after plating. Deposition of a BM is almost completed. Vacuoles (filled gray arrows) develop in the cytoplasm. (**D–G**) Cross section through a capillary that has developed in a fibrin hydrogel within 15 days. (**D**) Laminin 1 + 2 staining reveals the deposition of a BM. (**E**) CD31 immunofluorescence. (**F**) Nuclear Hoechst staining. (**G**) Merger of (**D–F**). (**H**) The polarized apical domains (AD) of three individual cells line the lumen (L) that develops in the intercellular space. Lumen-forming HuMECs contain several vacuoles (v). The lumen is always free of extracellular material. The basal domain (BD) of the cells faces the extracellular matrix of the hydrogel. No mesenchymal cells can be detected. A BM (black arrow) is deposited, see magnified inset. (**I**) A completely lumenized vascular structure is evident (indicated by the dotted line). The nucleus still protrudes into the capillary lumen. At a later stage of capillary development, the nucleus will completely retract to the capillary plasma membrane. Scale bars 10 μm. Color images available online at www.liebertonline.com/ten.

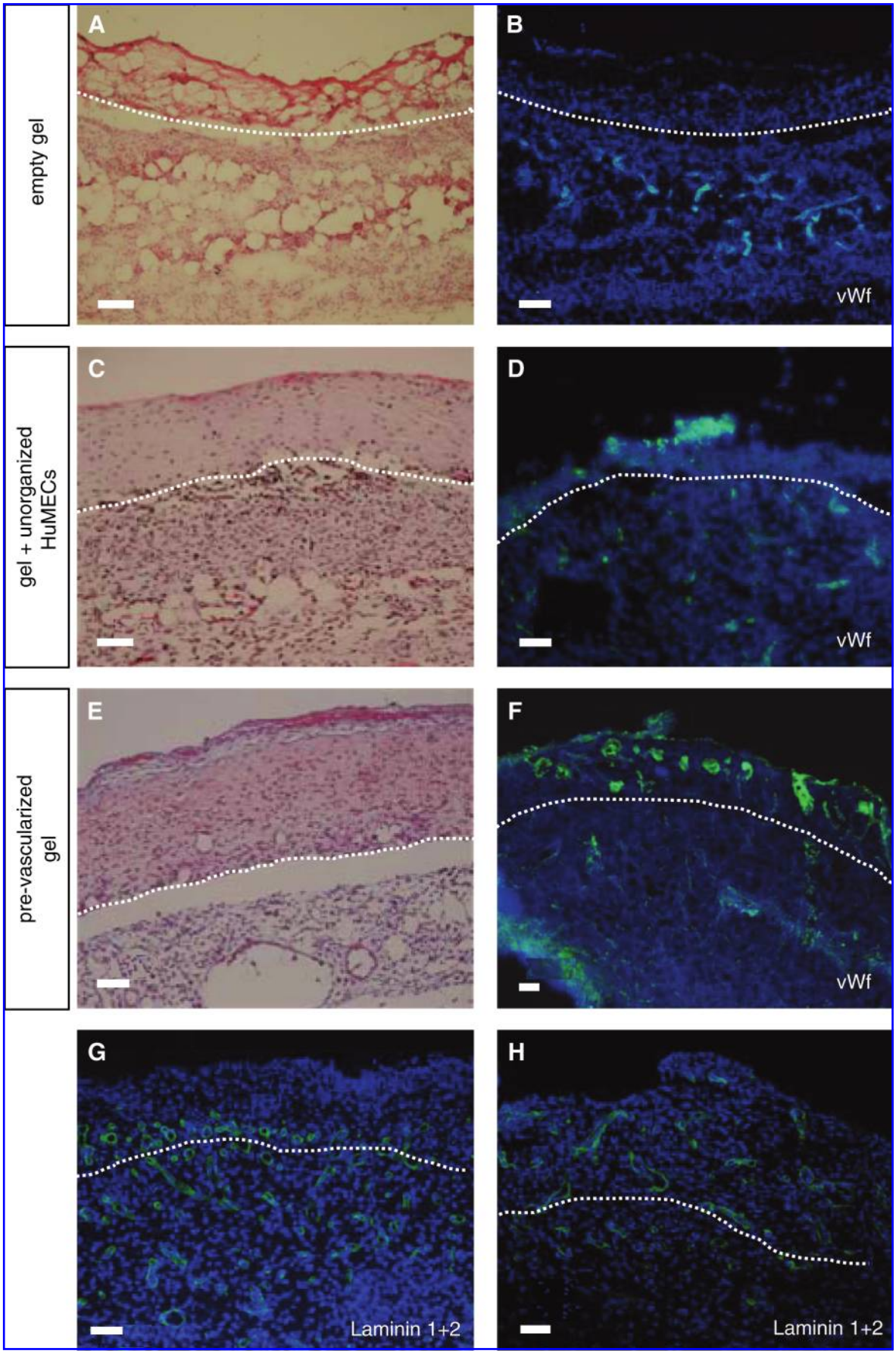
empty gel
gel + unorganized HuMECs
pre-vascularized gel
A
B
vWf
C
D
vWf
E
F
vWf
G
Laminin 1+2
H
Laminin 1+2

transplantation (Fig. 6A). The adjacent rat mesenchyme seemed to be unresponsive to the transplant, exhibiting only a moderate cellularity (Fig. 6A). However, already 5 days after transplantation, about one-third of the initially acellular gels was populated by cells derived from the underlying rat tissue (Fig. 6B). No vascular structures were detectable in these gels at this stage. Interestingly, gels containing the randomly distributed single HuMECs induced cell accumulation in the underlying rat mesenchyme (Fig. 6C). However, differentiated vWf-positive vascular structures were not detected in these gels (Fig. 6D). In contrast, prevascularized gels were densely populated by cells. They were in close contact with a dense, vascularized dermal mesenchyme (Fig. 6E). The thickness of the gels after transplantation adapted to about 150–200 μm. There was dehydration of the gels followed by degradation of fibrin and deposition of dermal matrix components, as soon as fibroblasts of the recipient animal populated the gels (data not shown).

As expected, prevascularized grafts exhibited numerous vWf-positive vascular structures (Fig. 6F). At 2 weeks after transplantation, gels containing single HuMECs showed only few vascular structures of rat origin. These had just started to penetrate into the fibrin matrix (neovascularization) (Fig. 6G). In contrast, the prevascularized gels had already long developed more differentiated vessels within the transplanted (engineered) area (Fig. 6H).

The human origin of vessels in 19 days old prevascularized transplants was confirmed using a primate-specific Alu probe. In Figure 7A it is confirmed that the Alu probe binds to nuclei of human cells, but does not hybridize to rat DNA (data not shown). Similarly an antibody to human CD31 (anti-human PECAM) made engineered capillaries of human origin visible (Fig. 7B). Costaining of human CD31 and a smooth muscle α-actin–specific antibody showed that most of the transplanted human capillaries were stabilized by α-actin–positive mural cells. (Fig. 7C). The antibody directed to smooth muscle α-actin was not rat specific, it also recognized the human protein. However, these mural cells were most likely of rat origin, since mural cells were neither detectable on cell culture plastic during the expansion phase nor could they be recognized on engineered capillaries *in vitro*. This mechanism of capillary stabilization may regulate the density of vascular structures in a given developing or regenerating tissue.

## Discussion

Successful transplantation of engineered tissues vitally depends on rapid and adequate blood supply. Our goal was to produce a prevascularized tissue substitute suitable for transplantation. In particular we aimed at providing the graft with a functioning capillary network that rapidly connects to the recipient's vascular system and thus allows timely perfusion and graft survival.

We show here that a network of branching and continuously lumenized capillaries can be produced *in vitro* and that prevascularization of tissue substitutes (derived from fibrin hydrogels) is demanding but possible. Fibrin has been demonstrated to be angiogenic *in vivo* and to support angiogenesis in 3D models *in vitro*.[17–19] In contrast, more light has to be shed on the vasculogenic properties of fibrin *in vitro*. Evidence for tube formation in fibrin is very limited.[20–22]

We show here that simple capillaries can develop in fibrin-based hydrogels from single dermal endothelial cells. Endothelial cells arrange into networks of lumenized capillaries within 15 to 21 days. The great number of capillaries may perhaps develop just by proliferation and differentiation of committed (nonprecursor) endothelial cells that remain functional for an extended period of time. In this case these structures would not self-renew and thus disappear with time. We therefore consider it much more likely that endothelial progenitor cells (EPCs), present in our initial cell preparations, give rise to *de novo* developing vascular structures. With the described culture system in our hands, we are now in the position to determine from which tissue source the EPCs are derived.

Based on the consideration that single EPCs may give rise to the genesis of new capillaries, one may argue that the process of capillary formation *in vitro* shows typical characteristics of vasculogenesis. Thus, in accordance to the reports from other investigators who looked into neovascularization,[23–26] our findings suggest that the genesis of new blood vessels *in vitro* may not be restricted to angiogenesis, but may also involve vasculogenesis.

The transparency of the hydrogels used in our experiments allowed documentation of the distinct steps of capillary formation. To our knowledge documentation of the genesis of capillaries has rarely been shown before in this clarity and

**FIG. 6.** Transplantation of three different types of hydrogels onto immunoincompetent rats: (1) gels without HuMECs, (2) gels with single, unorganized HuMECs, (3) prevascularized gels (**A–F**). Gels, 5 days after transplantation. (**A**) HE staining reveals the thickness and structure of the fibrin gel that did not contain cells before transplantation. The lower edge of the gel is marked by a white dotted line. The underlying mesenchyme seems to be unresponsive to the transplant, exhibiting only moderate cellularity. (**B**) Hoechst staining of a parallel section of the gel shown in (**A**) uncovers that the lower one-third of the gel is populated by rat cells, derived from the wound bed. The surface of the gel is apparently covered by a layer of rat cells that were contained in the wound fluid contacting the surface of the gel after its transplantation. No angiogenic structures are detected yet in these gels, using an antibody to von Willebrand factor (vWF). (**C**) Gels containing randomly distributed single HuMECs are thicker and obviously induce the underlying rat mesenchyme 5 days after transplantation. (**D**) However, differentiated vWf-positive angiogenic structures cannot be detected yet in the transplanted hydrogels. In a few spots endothelial cells have arranged into aggregates. (**E**) The prevascularized gel is about 200 m thick. As expected, it exhibits a high degree of cellularity. It obviously induces a dense dermal mesenchyme. (**F**) Prevascularized grafts exhibit numerous vWF-positive vessels in the engineered part. (**G, H**) Gels 2 weeks after transplantation. (**G**) Gels containing single unorganized HuMECs show only few blood vessels of rat origin that are just entering the transplanted fibrin matrix (neovascularization), as revealed by the use of laminin 1 + 2 specific antibodies. **(H)** In contrast, prevascularized gels contain vessels of progressed differentiation throughout the transplanted graft. All scale bars 50 μm. Color images available online at www.liebertonline.com/ten.

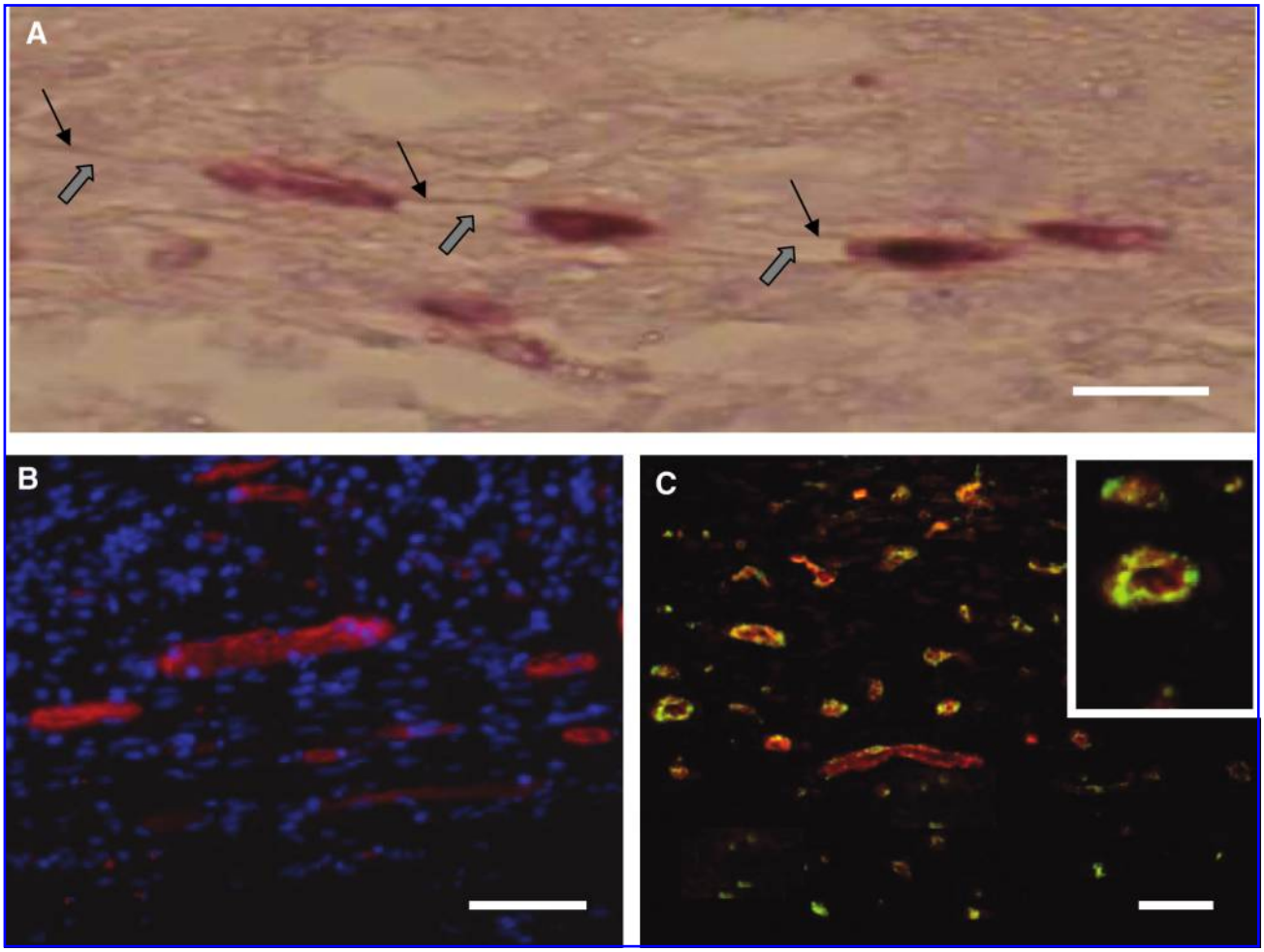


**FIG. 7.** Engineered human capillaries are stabilized by mural cells of rat origin. (**A**) The human origin of the vessels in the prevascularized transplants is confirmed by *in situ* hybridization using a DNA probe that specifically recognizes primate-specific Alu sequences. The figure shows four nuclei of human origin in a histological section through one fully lumenized capillary that developed within 19 days in the hydrogel. The lumen is indicated by gray arrows. Black arrows point to the plasma membrane. (**B**) Similarly an antibody to human CD31 (anti-human PECAM) reveals engineered capillaries of human origin (red fluorescence) 20 days after transplantation of the prevascularized graft onto a rat wound. (**C**) Costaining of human CD31 and rat smooth muscle α-actin 20 days after transplantation shows that most of the transplanted vessels of human origin are stabilized by α-actin–positive mural cells, such as pericytes and vascular smooth muscle cells. Smooth muscle α-actin-positive cells are most likely of rat origin, since they were extremely rare and could not be maintained in our EC cultures. Scale bar in (**A**) 10 μm, and in (**B**) and (**C**) 50 μm. Color images available online at www.liebertonline.com/ten.

quality. Our light and electron microscopical data show that two developmental steps are absolutely required to bring about capillary formation. These are the invagination of vesicles from the plasma membrane, referred to as pinocytosis and the deposition of a BM. Pinocytosis of membrane-bounded (bounded is bordered) vesicles appears to be an early step in capillary lumen formation. These vesicles coalesce to form a large vacuole within the intercellular space that fuses with the vacuoles of neighboring cells to establish luminal continuity. If this model of vascular tube formation is correct, then formation and targeting of apical membrane vesicles lie at the heart of the mechanism of tube formation. A prerequisite for that is the deposition of a uniform circumferential BM, which crucially guides the establishment of a radial polarity axis and finally stabilizes the growing microvessel.[27,28]

In its simplest manner, vascular development involves the following processes: formation, branching, sprouting, stabilization, remodeling and pruning, and specialization. We show here that capillary formation, branching, and sprouting can be achieved *in vitro*. We demonstrate that the timing of these processes overlaps.

We have developed a technique to facilitate endothelial cell extraction from dermal microvasculature. Fibroblasts contaminated our endothelial cell cultures in low numbers (if at all). Thus, in contrast to reports on the formation of vascular structures by HUVECs that require supporting fibroblasts and keratinocytes,[12,29] we show that human capillaries derived from dermal HuMECs can form and differentiate *in vitro* without the support of mural cells (pericytes, smooth muscle cells) or any other cell type. It remains to be investigated whether the two distinct sources of ECs are relevant in this respect.

After transplantation, the differentiation process of the *in vitro* generated vascular structures continues by the at-

traction of mural cells, which are known to support stabilization and maturation of capillaries.[28,30] The developing capillary network extends throughout the thickness of the hydrogel.

We found repeatedly that there is rapid vascularization after prevascularized matrices were transplanted onto immunoincompetent rats. However, the exact mechanism of inosculation, and of the interaction of vessels of the wound bed of the recipient animal with preformed vessels in the transplant, still remains to be worked on in more detail.

### Acknowledgments

We thank Andreas Zisch and Robert Friis for their valuable comments and for proofreading the manuscript. This work was supported by a grant from the European Union (EuroSTEC: LSHB-CT-2006-037409) and by the University of Zurich. We are particularly grateful to the Fondation Gaydoul, and the sponsors of Dona Tissue (Thérèse Meier and Robert Zingg), the vonTobel Foundation, and the Werner Spross Foundation for their financial support and their interest in our work.

### Disclosure Statement

No competing financial interests exist.

### References

1. Nomi, M., Atala, A., Coppi, P.D., and Soker, S. Principals of neovascularization for tissue engineering. Mol Aspects Med **23,** 463, 2002.
2. Tremblay, P.L., Hudon, V., Berthod, F., Germain, L., and Auger, F.A. Inosculation of tissue-engineered capillaries with the host's vasculature in a reconstructed skin transplanted on mice. Am J Transplant **5,** 1002, 2005.
3. Byrne, G.W., Schirmer, J.M., Fass, D.N., Teotia, S.S., Kremers, W.K., Xu, H., Naziruddin, B., Tazelaar, H.D., Logan, J.S., and McGregor, C.G. Warfarin or low-molecular-weight heparin therapy does not prolong pig-to-primate cardiac xenograft function. Am J Transplant **5,** 1011, 2005.
4. Mai, G., Bucher, P., Morel, P., Mei, J., Bosco, D., Andres, A., Mathe, Z., Wekerle, T., Berney, T., and Buhler, L.H. Anti-CD154 mAb treatment but not recipient CD154 deficiency leads to long-term survival of xenogeneic islet grafts. Am J Transplant **5,** 1021, 2005.
5. Preston, E.H., Xu, H., Dhanireddy, K.K., Pearl, J.P., Leopardi, F.V., Starost, M.F., Hale, D.A., and Kirk, A.D. IDEC-131 (anti-CD154), sirolimus and donor-specific transfusion facilitate operational tolerance in non-human primates. Am J Transplant **5,** 1032, 2005.
6. Lattmann, T., Hein, M., Horber, S., Ortmann, J., Teixeira, M.M., Souza, D.G., Haas, E., Tornillo, L., Munter, K., Vetter, W., and Barton, M. Activation of pro-inflammatory and anti-inflammatory cytokines in host organs during chronic allograft rejection: role of endothelin receptor signaling. Am J Transplant **5,** 1042, 2005.
7. Young, D.M., Greulich, K.M., and Weier, H.G. Species-specific *in situ* hybridization with fluorochrome-labeled DNA probes to study vascularization of human skin grafts on athymic mice. J Burn Care Rehabil **17,** 305, 1996.
8. Supp, D.M., Karpinski, A.C., and Boyce, S.T. Vascular endothelial growth factor overexpression increases vascularization by murine but not human endothelial cells in cultured skin substitutes grafted to athymic mice. J Burn Care Rehabil **25,** 337, 2004.
9. Supp, D.M., and Boyce, S.T. Overexpression of vascular endothelial growth factor accelerates early vascularization and improves healing of genetically modified cultured skin substitutes. J Burn Care Rehabil **23,** 10, 2002.
10. Tonello, C., Vindigni, V., Zavan, B., Abatangelo, S., Abatangelo, G., Brun, P., and Cortivo, R. *In vitro* reconstruction of an endothelialized skin substitute provided with a microcapillary network using biopolymer scaffolds. Faseb J **12,** 1331, 2005.
11. Wu, X., Rabkin-Aikawa, E., Guleserian, K.J., Perry, T.E., Masuda, Y., Sutherland, F.W., Schoen, F.J., Mayer, J.E., Jr., and Bischoff, J. Tissue-engineered microvessels on three-dimensional biodegradable scaffolds using human endothelial progenitor cells. Am J Physiol Heart Circ Physiol **287,** H480, 2004.
12. Chen, X., Aledia, AS., Ghajar, CM., Griffith, CK., Putnam, AJ., Hughes, CC., and George, SC. Prevascularization of a fibrin-based tissue construct accelerates the formation of functional anastomosis with host vasculature. Tissue Eng Part A **15,** 1363, 2009.
13. Kaully, T., Kaufman-Francis, K., Lesman, A., and Levenberg, S. Vascularization—the conduit to viable engineered tissues. Tissue Eng Part B Rev **15,** 159, 2009.
14. Pontiggia, L. Markers to evaluate the quality and self-renewing potential of engineered human skin substitutes *in vitro* and after transplantation. J Invest Dermatol **129,** 480, 2009.
15. Just, L., Timmer, M., Tinius, J., Stahl, F., Deiwick, A., Nikkhah, G., and Bader, A. Identification of human cells in brain xenografts and in neural co-cultures of rat by *in situ* hybridization with Alu probe. J Neurosci Methods **126,** 69, 2003.
16. Lubarsky, B., and Krasnow, M.A. Tube morphogenesis: making and shaping biological tubes. Cell **112,** 19, 2003.
17. Xue, L., and Greisler, H.P. Angiogenic effect of fibroblast growth factor-1 and vascular endothelial growth factor and their synergism in a novel *in vitro* quantitative fibrin-based 3-dimensional angiogenesis system. Surgery **132,** 259, 2002.
18. Korff, T., and Augustin, H.G. Tensional forces in fibrillar extracellular matrices control directional capillary sprouting. J Cell Sci **112 (Pt 19),** 3249, 1999.
19. Uriel, S., Brey, E.M., and Greisler, H.P. Sustained low levels of fibroblast growth factor-1 promote persistent microvascular network formation. Am J Surg **192,** 604, 2006.
20. Tranqui, L., and Tracqui, P. Mechanical signalling and angiogenesis. The integration of cell-extracellular matrix couplings. C R Acad Sci **323,** 31, 2000.
21. Vailhe, B., Lecomte, M., Wiernsperger, N., and Tranqui, L. The formation of tubular structures by endothelial cells is under the control of fibrinolysis and mechanical factors. Angiogenesis **2,** 331, 1998.
22. Vailhe, B., Ronot, X., Tracqui, P., Usson, Y., and Tranqui, L. *In vitro* angiogenesis is modulated by the mechanical properties of fibrin gels and is related to alpha(v)beta3 integrin localization. In Vitro Cell Dev Biol Anim **33,** 763, 1997.
23. Brey, E.M., Uriel, S., Greisler, H.P., and McIntire, L.V. Therapeutic neovascularization: contributions from bioengineering. Tissue Eng **11,** 567, 2005.
24. Capla, J.M., Ceradini, D.J., Tepper, O.M., Callaghan, M.J., Bhatt, K.A., Galiano, R.D., Levine, J.P., and Gurtner, G.C. Skin graft vascularization involves precisely regulated regression and replacement of endothelial cells through both

angiogenesis and vasculogenesis. Plast Reconstr Surg **117,** 836, 2006.
25. Eguchi, M., Masuda, H., and Asahara, T. Endothelial progenitor cells for postnatal vasculogenesis. Clin Exp Nephrol **11,** 18, 2007.
26. Francis, M.E., Uriel, S., and Brey, E.M. Endothelial cell-matrix interactions in neovascularization. Tissue Eng **14,** 19, 2008.
27. Maisonpierre, P.C., Suri, C., Jones, P.F., Bartunkova, S., Wiegand, S.J., Radziejewski, C., Compton, D., McClain, J., Aldrich, T.H., Papadopoulos, N., Daly, T.J., Davis, S., Sato, T.N., and Yancopoulos, G.D. Angiopoietin-2, a natural antagonist for Tie2 that disrupts *in vivo* angiogenesis. Science **277,** 55, 1997.
28. Metheny-Barlow, L.J., and Li, L.Y. The enigmatic role of angiopoietin-1 in tumor angiogenesis. Cell Res **13,** 309, 2003.
29. Black, A.F., Berthod, F., L'Heureux, N., Germain, L., and Auger, F.A. *In vitro* reconstruction of a human capillary-like network in a tissue-engineered skin equivalent. Faseb J **12,** 1331, 1998.
30. Armulik, A., Abramsson, A., and Betsholtz, C. Endothelial/pericyte interactions. Circ Res **97,** 512, 2005.

Address correspondence to:
*Ernst Reichmann, Ph.D.*
*Tissue Biology Research Unit*
*Department of Surgery*
*University Children's Hospital*
*University of Zurich*
*Steinwiesstrasse 75*
*CH-8032 Zurich*
*Switzerland*

*E-mail:* ernst.reichmann@kispi.uzh.ch

*Received: October 2, 2008*
*Accepted: August 24, 2009*
*Online Publication Date: October 27, 2009*